Galectin-9 inhibits TLR7-mediated autoimmunity in murine lupus models

Santosh K. Panda,[1,2] Valeria Facchinetti,[3] Elisaveta Voynova,[1] Shino Hanabuchi,[1,2] Jodi L. Karnell,[1] Richard N. Hanna,[1] Roland Kolbeck,[1] Miguel A. Sanjuan,[1] Rachel Ettinger,[1] and Yong-Jun Liu[1,2,3]

[1]MedImmune, Gaithersburg, Maryland, USA. [2]Baylor Institute for Immunology Research, Dallas, Texas, USA. [3]MD Anderson Cancer Center, Houston, Texas, USA.

Uncontrolled secretion of type I IFN, as the result of endosomal TLR (i.e., TLR7 and TLR9) signaling in plasmacytoid DCs (pDCs), and abnormal production of autoantibodies by B cells are critical for systemic lupus erythematosus (SLE) pathogenesis. The importance of galectin-9 (Gal-9) in regulating various autoimmune diseases, including lupus, has been demonstrated. However, the precise mechanism by which Gal-9 mediates this effect remains unclear. Here, using spontaneous murine models of lupus (i.e., BXSB/MpJ and NZB/W F1 mice), we demonstrate that administration of Gal-9 results in reduced TLR7-mediated autoimmune manifestations. While investigating the mechanism underlying this phenomenon, we observed that Gal-9 inhibits the phenotypic maturation of pDCs and B cells and abrogates their ability to mount cytokine responses to TLR7/TLR9 ligands. Importantly, immunocomplex-mediated (IC-mediated) and neutrophil extracellular trap–mediated (NET-mediated) pDC activation was inhibited by Gal-9. Additionally, the mTOR/p70S6K pathway, which is recruited by both pDCs and B cells for TLR-mediated IFN secretion and autoantibody generation, respectively, was attenuated. Gal-9 was found to exert its inhibitory effect on both the cells by interacting with CD44.

Introduction

Systemic lupus erythematosus (SLE) is a chronic autoimmune disorder associated with complex pathologies, such as glomerulonephritis, arthritis, and skin lesions. Disease pathogenesis in SLE is attributed to high levels of IFN-α and autoantibodies (1), both of which positively correlate with severity of pathosis (2). Autoantibodies and self-nucleic acids form immunocomplexes (ICs), which are deposited in various organs with resultant inflammation and tissue damage (3). Loss of tolerance against self-nuclear antigens induces hyperactivation of plasmacytoid DCs (pDC) and B cells through nucleic-acid sensing TLR7 and TLR9 and drives production of type-1 IFN and anti-nuclear autoantibodies (1). Type-1 IFN directly primes autoreactive B and T cells and also induces DC-mediated autoreactive T cell activation, resulting in augmentation of autoimmunity (4, 5).

pDCs are bone marrow–derived professional type I IFN-producing cells (6). Upon recognition of viral and bacterial nucleic acids through endosomal TLR7 and TLR9, pDCs rapidly produce a massive amount of type I IFNs and subsequently mature into DCs to trigger the adaptive immune response (7, 8). Uncontrolled chronic secretion of IFN-α in response to self-nuclear antigens, however, is associated with the development of autoimmune disorders, such as psoriasis and SLE (9). Self-nucleic acids complexed with autoantibodies or DNA-binding proteins, such as LL37 or high mobility group box 1 (HMGB1), activate pDCs and induce type I IFN production through TLR7 and TLR9 (9). In addition, neutrophil extracellular traps (NETs) containing self-DNA complexes released from dying neutrophils are also major triggers of TLR7/TLR9-mediated pDC activation and IFN-α production during SLE pathogenesis (10). Recently, 2 groups independently demonstrated that ablation of pDCs in experimental lupus models results in disease amelioration (11, 12), further suggesting the importance of TLR7 and TLR9 signaling in lupus.

TLR7 and TLR9 signaling in B cells also plays an important role in the initiation and progression of lupus. TLR7 and IFN-α act synergistically to promote generation of pathogenic IgG2a and IgG2c isotypes through class-switch recombination (1, 13). Overexpression of TLR7 has been shown to induce lupus manifestations, while deletion or downregulation of the gene is protective against lupus (14). TLR9/MyD88 signaling provides costimulatory signals for pathogenic autoantibody production by autoreactive B cells (15). The above studies strongly suggest that TLR7/TLR9 signaling is pivotal in SLE pathogenesis and hence is regarded as an important target for therapeutic intervention.

Galectin-9 (Gal-9) is a conserved s-type lectin that has a tandem repeat of 2 carbohydrate-recognition domains (CRDs) and is highly expressed in various tissues, including lymph nodes, bone marrow, liver, thymus, and spleen (16). It exhibits multiple immunomodulatory functions in both innate and adaptive immune responses. Gal-9 plays an antiinflammatory role by inducing apoptosis in activated T cells, inhibiting Th1 and Th17 responses, and promoting the differentiation of Tregs (17). Administration of Gal-9 reduces collagen-induced arthritis (CIA) and rheumatoid arthritis (RA) manifestations in mouse models (18, 19). Gal-9 has been shown to suppress experimental autoimmune encephalomyelitis (EAE) as well as IC-induced arthritis by manipulating the

Authorship note: SKP and VF, as well as RE and YJL, contributed equally to this work.
Conflict of interest: RE and JLK are currently employees at and shareholders at Viela Bio.
Submitted: September 6, 2017; **Accepted:** February 13, 2018.
Reference information: *J Clin Invest*. 2018;128(5):1873–1887.
https://doi.org/10.1172/JCI97333.

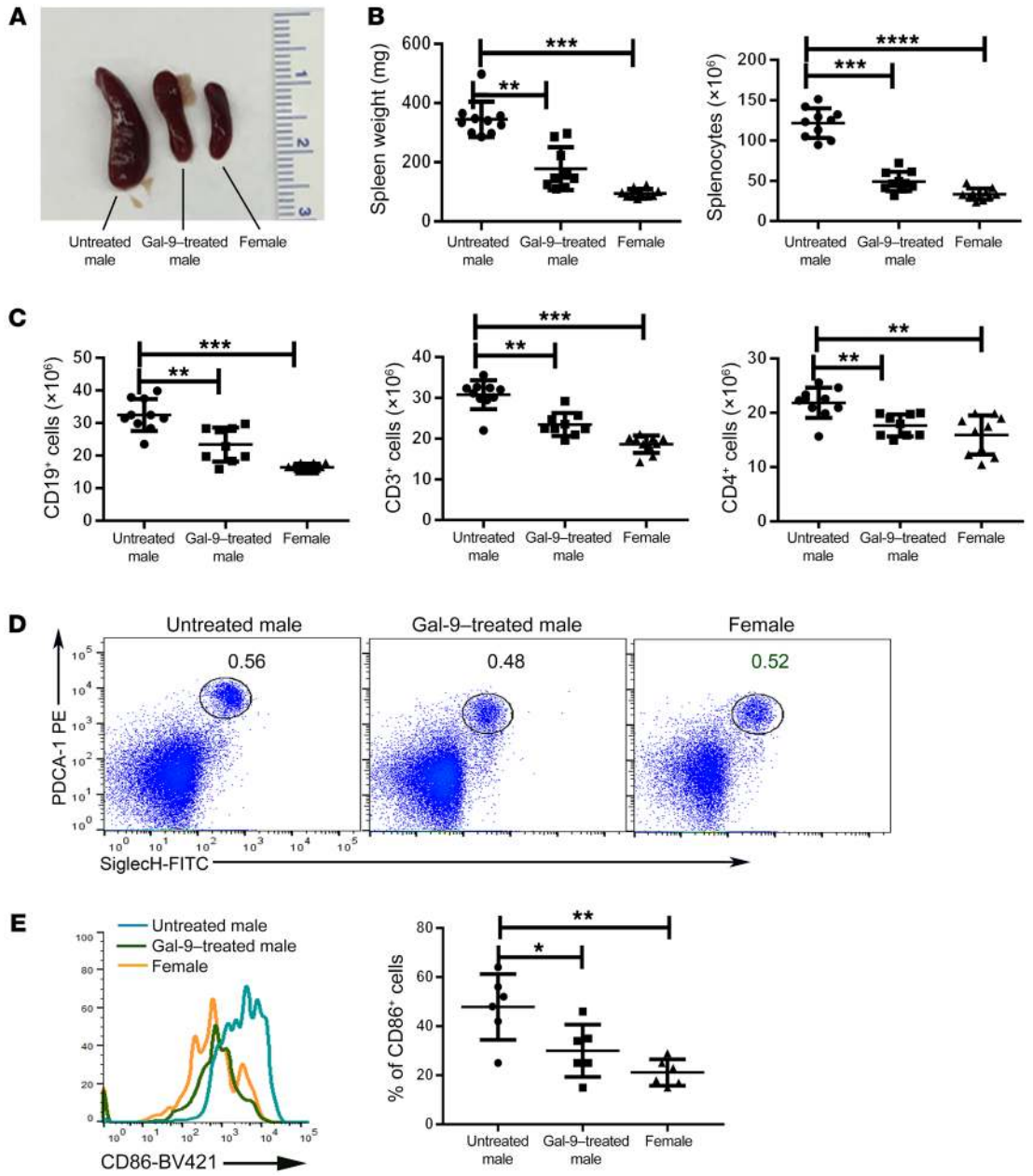

Figure 1. Splenomegaly and hyperplasia in the spleens of male BXSB/MpJ mice are inhibited with Gal-9 treatment. Male BXSB/MpJ mice were treated with Gal-9 from 8 to 18 weeks; the spleens were collected at 19 weeks and analyzed. (**A**) Representative images of the size of the spleens. (**B**) Histograms showing the weight of the spleens, the total number of splenocytes, (**C**) B cells (CD19⁺), T cells (CD3⁺), and T helper cells (CD4⁺). Data points represent individual mice. (**D**) Representative flow plots of pDC staining and the percentage of pDCs in the spleens of Gal-9–treated males and untreated male and female littermates. (**E**) A representative histogram of the expression of CD86 on pDCs and percentage of CD86-expressing pDCs of Gal-9–treated males, untreated males, and female littermates. Data are shown as mean ± SD. $n = 10$. Data are representative of 2 independent experiments. One-way ANOVA with Dunnett's multiple comparison was used to test the statistical significance for all the data. For **E**, Kruskal-Wallis testing was performed, followed by Dunn's test. $^{*}P < 0.05$; $^{**}P < 0.01$; $^{***}P < 0.001$ versus control; $^{****}P < 0.0001$.

functions of T cells and macrophages (18). It was also demonstrated that Gal-9 diminishes the clinical severity of lupus in MRL/lpr lupus-prone mice (20); however, whether Gal-9 exerts its effect on lupus pathogenesis by influencing TLR7/TLR9 signaling and, if it does, identification of the precise mechanism underlying this phenomenon, has yet to be addressed.

In order to investigate the effect of Gal-9 on TLR7 signaling, we utilize BXSB/MpJ (having Yaa mutation), a spontaneous animal model of lupus in which autoimmunity is induced by overexpression of TLR7 (21). Y-linked autoimmune accelerator–associated (Yaa-associated) duplication of 19 genes, including TLR7, results in development of autoimmune disorder in BXSB male mice. We also employed NZB/W F1 mice, in which, in females, TLR7/TLR9 signaling plays an important role in the development of lupus pathogenesis (11). The disease manifestation starts around 8 weeks in BXSB/MpJ male mice, whereas female NZB/W F1 mice exhib-

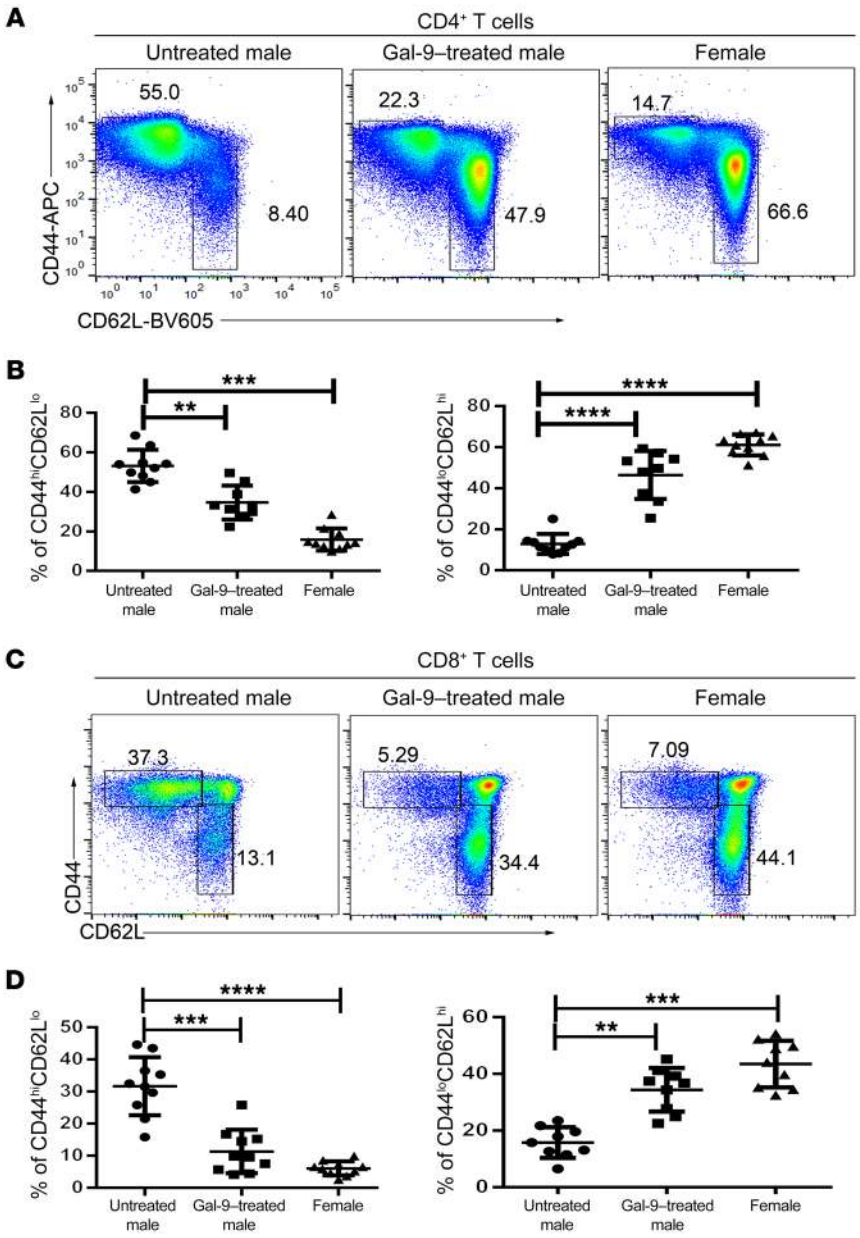

Figure 2. Administration of Gal-9 impairs the expansion and activation of T cells. Splenocytes from male BXSB/MpJ mice with and without Gal-9 treatment and female littermates of 19 weeks of age were analyzed. Representative flow cytometric figures of the expression of CD44 and CD62L on $CD4^+$ T cells (**A**) and $CD8^+$ T cells (**C**). Frequency of $CD44^{hi}CD62L^{lo}$ and $CD44^{lo}CD62L^{hi}$ cells on $CD4^+$ T cells (**B**) and $CD8^+$ T cells (**D**), as analyzed by flow cytometry. Data points represent individual mice. $n = 10$. Data are representative of 2 independent experiments and are shown as mean ± SD. One-way ANOVA with Dunnett's multiple comparison was used to test statistical significance. $^*P < 0.05$; $^{**}P < 0.01$; $^{***}P < 0.001$ versus control; ****P < 0.0001.

it clinical parameters of lupus at around 15 to 17 weeks. Both the models recapitulate the splenomegaly, lymphadenopathy, proliferative glomerulonephritis, and increased levels of autoantibodies against nuclear antigens observed in clinical SLE.

In this study, we have demonstrated that administration of Gal-9 in the early stage of the disease reduced splenomegaly, activation and expansion of T and B cells, and autoantibody generation and alleviated kidney pathology in lupus-prone BXSB/MpJ and NZB/W F1 mice. TLR7/TLR9-mediated activation and maturation of pDC and B cells was inhibited by Gal-9. Importantly, Gal-9 impaired IC- and NET-triggered pDC activation. Mechanistically, Gal-9 disrupted the TLR-mediated mTOR/p70S6K pathway, which is required for IFN production and autoantibody generation by pDC and B cells, respectively. Together, our findings demonstrate that Gal-9 ameliorates lupus pathogenesis by inhibiting endosomal TLR signaling.

Results

Administration of Gal-9 inhibited splenomegaly in BXSB/MpJ mice. Gal-9 was administered to male BXSB/MpJ mice at the early onset of lupus pathogenesis, and several disease parameters were analyzed at 19 weeks of age. Untreated male and female littermates were used as controls. Administration of Gal-9 resulted in reduced splenomegaly as compared with that in untreated controls (Figure 1, A and B). The decrease in spleen size was attributed to reduced cellular hyperplasia in the spleen. The number of B cells ($CD19^+$), T cells ($CD3^+$), and T helper cells ($CD4^+$) in the spleen was significantly decreased in Gal-9–treated mice as compared with untreated male mice and was comparable to that in healthy female littermates that do not develop the disease (Figure 1C). Importantly, Gal-9 did not reduce the size of the pDC population (Figure 1D), but rather inhibited pDC activation, as shown by reduced surface expression of CD86 upon treatment (Figure 1E).

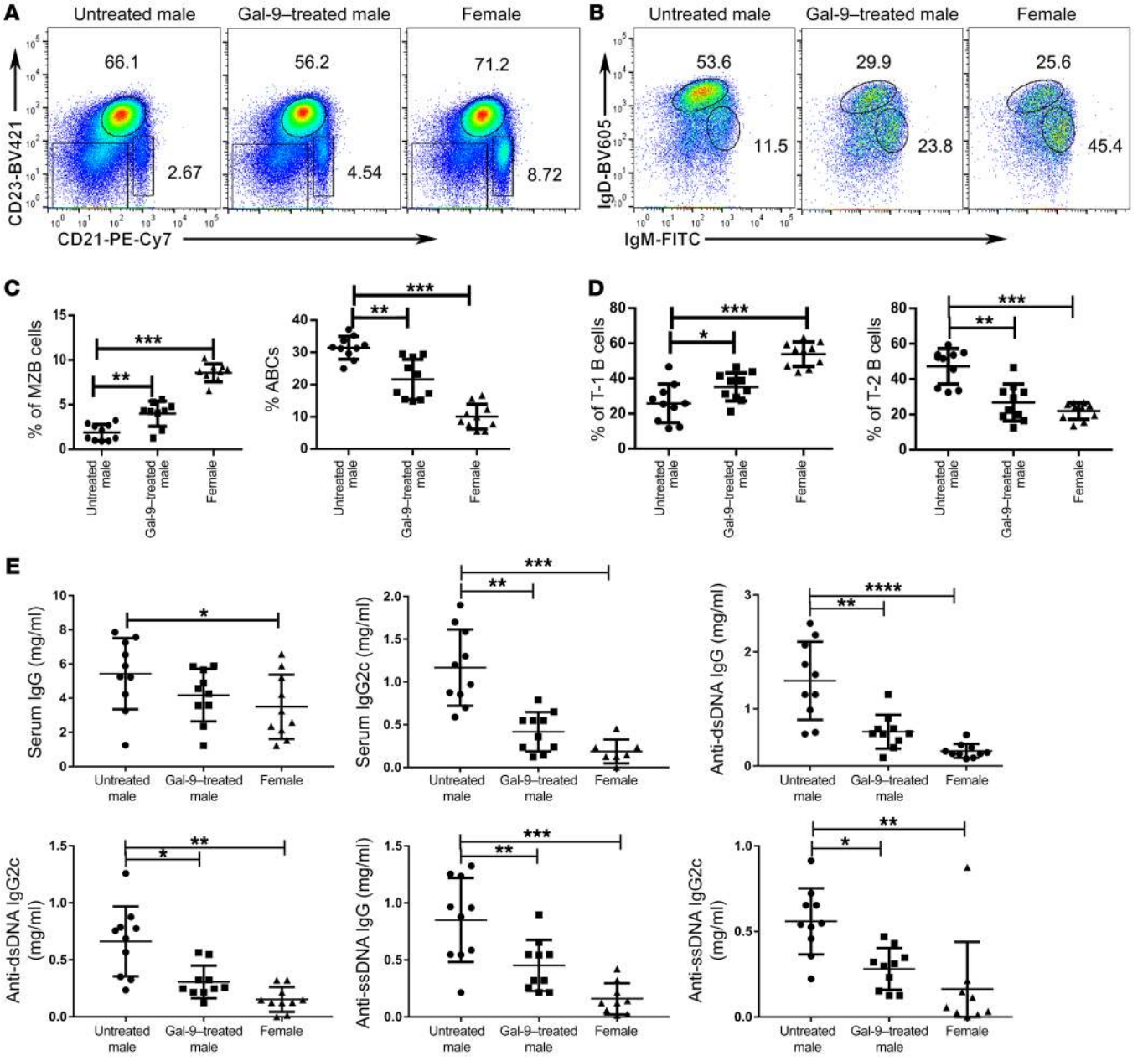

Figure 3. Gal-9 administration inhibits ABC and T2B cell expansion, reconstitutes MZB and T1 B cells, and limits autoantibody generation in male BXSB/MpJ mice. Splenocytes from Gal-9–treated male, untreated male, and age-matched female littermates were analyzed for expression of different markers on CD19$^+$ B cells. (**A**) Representative flow plots of CD23 and CD21 expression on splenic B cells. (**B**) Frequency of CD23$^-$CD21^{hi} MZB cells and CD23$^-$CD21$^-$AA4.1$^-$ ABCs were analyzed by FACS. (**C**) Representative graphs of (CD21$^-$, CD23$^-$, IgM$^+$, and IgD^{lo}) T1 cells and (CD21$^-$, CD23$^-$, IgM$^+$, and IgD^{hi}) T2 cells. (**D**) Frequency of T1 cells and T2 cells was analyzed by FACS. Data points represent individual mice. Data are shown as mean ± SD. (**E**) Serum of male BXSB/MpJ mice treated with Gal-9 along with untreated control and age-matched female littermates were analyzed for levels of IgG and IgG2c against nuclear autoantigens by ELISA. Data points represent individual mice. n = 10. Data are representative of 2 independent experiments and are shown as mean ± SD. One-way ANOVA with Dunnett's multiple comparison was used to test the statistical significance for data presented in **C** and **D**, and Kruskal-Wallis testing was performed followed by Dunn's test for **E**. *P < 0.05; **P < 0.01; ***P < 0.001 versus control; ****P < 0.0001.

Aberrant expansion and activation of T cells during lupus is inhibited by Gal-9 treatment. Hyperactivation and expansion of T cells are characteristics of lupus. In order to evaluate the effect of Gal-9 on T cell populations, we analyzed splenic T cells in Gal-9–treated male and untreated male and female littermates. The frequencies of the activated CD4$^+$ and CD8$^+$ T cell populations (CD44^{hi} and CD62L^{lo}) were greatly increased in untreated male mice compared with healthy female littermates. We found that the number of activated CD4$^+$ and CD8$^+$ T cells was dramatically reduced upon Gal-9 treatment in male mice (Figure 2, A–D). The reduction of activated CD44^{hi} T cells was correlated with an increased number of CD44^{lo}CD62L^{hi} resting T cells in Gal-9–treated male mice (Figure 2, A–D). CD69^{hi}CD62L^{lo} activated CD4$^+$ and CD8$^+$ T cells were also downregulated upon Gal-9 treatment (Supplemental Figure 1, A–D;

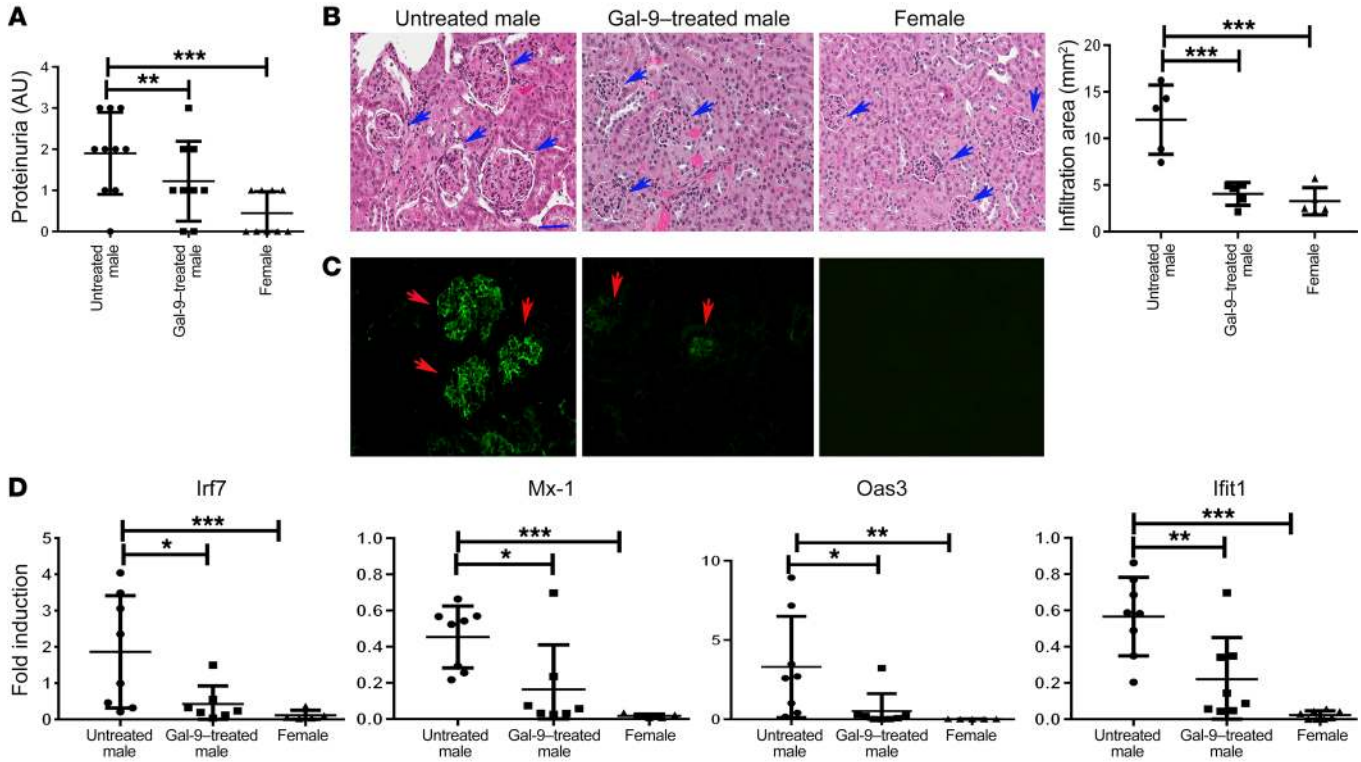

Figure 4. Gal-9 administration ameliorates severity of kidney pathology. Proteinuria of both Gal-9–treated and untreated control male BXSB/MpJ mice along with female littermates is shown (**A**) (n = 9). Formalin-fixed kidney sections from 19-week-old Gal-9–treated and untreated control male BXSB/MpJ mice along with female littermates were stained for H&E. Frozen kidney sections were stained for IgG. Representative images of 5 animals in each group (**B** and **C**). Individual glomeruli are marked with arrows. Original magnification, ×10. Relative expression of IFN-induced genes in kidney tissue was analyzed by reverse-transcriptase PCR (RT-PCR) (**D**). Data points indicate individual mice. Data are representative of 2 independent experiments. Kruskal-Wallis testing was performed, followed by Dunn's test for statistical significance. *$P < 0.05$; **$P < 0.01$; ***$P < 0.001$ versus control.

supplemental material available online with this article; https://doi.org/10.1172/JCI97333DS1), whereas no difference in the $CD4^+$ $Foxp3^+$ Treg profile was observed (Supplemental Figure 2).

Gal-9 administration limits abnormal B cell activation and expansion. Abnormal activation and expansion of multiple B cell subsets play a central role in the development and progression of SLE pathogenesis. Loss of marginal zone B (MZB) cells, expansion of age-associated B cells (ABCs) and transitional stage 2 B (T2B) cells, and low transitional stage 1B (T1B) cells have been demonstrated in clinical and experimental conditions of lupus (11). It has been reported that male BXSB/MpJ mice lose $CD23^-$ $CD21^{hi}$ MZB cells during development of the disease (11). We observed that these MZBs, which were lost in untreated control male mice due to lupus, were partially restored upon treatment with Gal-9 (Figure 3, A and C).

ABCs are an unusual cell population that is present in aging individuals and in women with autoimmune disorders (11). It has been shown that ABCs ($CD23^-$, $CD21^-$, $AA4.1^-$) accumulated in several mouse models of autoimmune diseases, including the BXSB/MpJ mice, in a pDC-dependent manner (11). We therefore analyzed this cell population in untreated males, Gal-9–treated males, and healthy female littermates. The number of ABCs was significantly reduced upon Gal-9 treatment (Figure 3C). We also observed a partial recovery of the T1B cell ($CD19^+$, $CD21^-$, $CD23^-$, IgM^+, and IgD^{lo}) population in Gal-9–treated mice as compared with untreated male mice (Figure 3, B and D), whereas the T2B ($CD19^+$, $CD21^-$, $CD23^-$, $IgM^{-/lo}$, and IgD^{hi}) cell population was reduced to the level of healthy females upon Gal-9 treatment (Figure 3, B and D).

We analyzed the profile of autoantibodies in the serum of Gal-9–treated BXSB/MpJ mice. Total IgG levels between Gal-9–treated male and untreated male and female groups remained comparable (Figure 3E), whereas the levels of pathogenic IgG2c antibodies decreased upon Gal-9 treatment. IgG and IgG2c antibodies against nuclear autoantigens, such as dsDNA, ssDNA, and chromatin, were reduced upon Gal-9 treatment (Figure 3E and data not shown). These data suggest that Gal-9 treatment inhibits pathogenic autoantibody production in experimental lupus.

Administration of Gal-9 suppresses the glomerulonephritis and IFN signatures in the kidneys of male BXSB/MpJ mice. We next analyzed proteinuria and kidney histology to determine the effect of Gal-9 on renal pathology, the most complicated form of lupus manifestation. BXSB/MpJ male mice had high proteinuria levels compared with untreated healthy female littermates. In contrast, the Gal-9–treated group exhibited low proteinuria levels (Figure 4A). Glomerular membrane thickening and glomerular hypercellularity as well as IC deposition were reduced in male mice upon Gal-9 treatment (Figure 4, B and C). Marked signatures of IFN-α/β–induced genes are positively correlated with lupus disease activity (22). We observed reduced expression of IFN-induced genes, such as Mx-1, Oas-3, Irf-7, and Ifit-1,

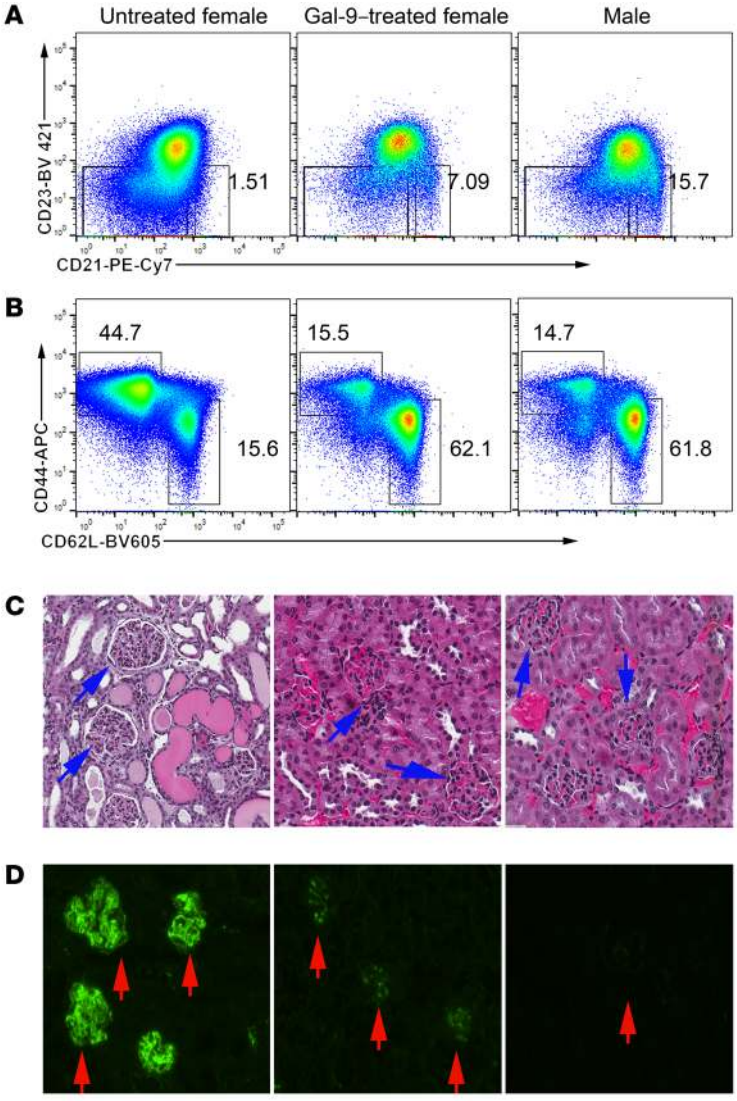

Figure 5. Gal-9 administration reduces lupus pathogenesis in NZB/W F1 mice. Splenocytes from Gal-9–treated female, untreated female, and age-matched male littermates of NZB/W F1 mice were analyzed for expression of different markers on CD19$^+$ B cells and CD3$^+$ T cells. (**A**) Representative flow cytometric plots of CD23 and CD21 expression on splenic B cells. (**B**) Representative flow cytometric plots of the expression of CD44 and CD62L on splenic CD4$^+$ T cells. (**C**) Formalin-fixed kidney sections from 32-week-old Gal-9–treated and untreated control female along with male littermates were stained for H&E. (**D**) Frozen kidney sections were stained for IgG. Representative images of 5 animals in each group. Individual glomeruli are marked with arrows. Original magnification, ×10.

in the kidneys of Gal-9–treated mice (Figure 4D). Together, these findings suggest that TLR7-mediated kidney pathologies are abrogated by Gal-9.

Gal-9 reduces lupus-associated clinical parameters in NZB/W F1 mice. Although BXSB/MpJ mice mimic clinical lupus by exhibiting high titers of anti-nuclear autoantibodies, overt glomerulonephritis, and expression of IFN signatures, disposition of male mice to lupus is opposite of that of clinical SLE, in which females are more susceptible. Hence, we employed another spontaneous model of lupus, NZB/W F1, in which female mice develop a lupus-like autoimmune disorder. Gal-9 was administered from 20 weeks to 31 weeks of age, and immunological parameters related to lupus were analyzed at the end of the treatment. Reduced splenomegaly and cellular hyperplasia were observed in Gal-9–treated female mice as compared with untreated females (data not shown). Lowered splenic MZB cells due to lupus were partially restored upon Gal-9 administration (Figure 5A and Supplemental Figure 3A). Additionally, Gal-9 treatment reduced frequency of activated (CD44^{hi} and CD62L^{lo}) CD4$^+$ and CD8$^+$ T cells (Figure 5B, Supplemental Figure 3B, and data not shown). Similarly, CD69 expression on CD4$^+$ and CD8$^+$ T cells was reduced (data not shown). Importantly, proteinuria, glomerular nephritis, and IC deposition on the kidneys of female mice were reduced by Gal-9 treatment (Figure 5, C and D, and Supplemental Figure 3C). Gal-9 treatment also reduced pathogenic IgG and IgG2a autoantibodies against nuclear antigens (Supplemental Figure 3D).

Therapeutic effect of Gal-9 on lupus. The strong prophylactic effect of Gal-9 on lupus manifestations in both BXSB/MpJ and NZB/W F1 mice led us to investigate the potential therapeutic benefits of Gal-9. A group of BXSB/MpJ mice was administered Gal-9 at 14 weeks of age when clinical parameters, such as splenomegaly, increased frequency of activated T cells, and high titers of anti-nuclear autoantibodies, had emerged. Following 5 weeks of treatment in mice with established disease, Gal-9 neither reduced splenomegaly nor restored MZB cells, as was observed with prophylactic administration (Figure 6A, Supplemental Figure 4A, and data not shown). Interestingly frequency of activated CD4$^+$ and CD8$^+$ T cells was reduced upon late Gal-9 treatment (Figure 6B and Supplemental Figure 4B). Kidney pathologies were also marginally ameliorated upon late treatment with Gal-9 (Figure 6, C and D, and Supplemental Figure 4C). There was a marginal decrease in titers of IgG, whereas IgG2c autoantibody titers against dsDNA were comparable (Supplemental Figure 4D). These data demonstrate a limited/minimal role for Gal-9 in the modulation of established disease, suggesting that pathways regulated by Gal-9 are involved in the initiation of autoimmune manifestations.

Gal-9 inhibits TLR7/TLR9-mediated pDC functions. Lupus pathogenesis and the autoimmune response generated due to hyperexpression of TLR7 is ameliorated by ablation of pDCs (11, 12). Similarly, the TLR7/TLR9 inhibitors also downgrade lupus pathogenesis in NZB/W F1 mice (21). Since Gal-9 treatment reversed the clinical parameters of lupus similarly to pDC ablation and administration of TLR7/TLR9 inhibitor in BXSB/MpJ mice and NZB/W F1 mice, respectively, we hypothesized that Gal-9 acts on key regulators of lupus, such as pDC and TLR7 signaling. In order to understand whether Gal-9 plays a role in TLR-mediated pDC activation, nonautoimmune C57BL/6 mice were injected with CpG-A along with Gal-9 and plasma levels of IFN-α were analyzed after 6 hours. Serum levels of IFN-α induced by CpG-A were reduced by Gal-9 (Figure 7A), suggesting that Gal-9 inhibits pDC functions. To investigate the direct function of Gal-9 on pDCs, we stimulated freshly isolated murine (C57BL/6) pDCs with various

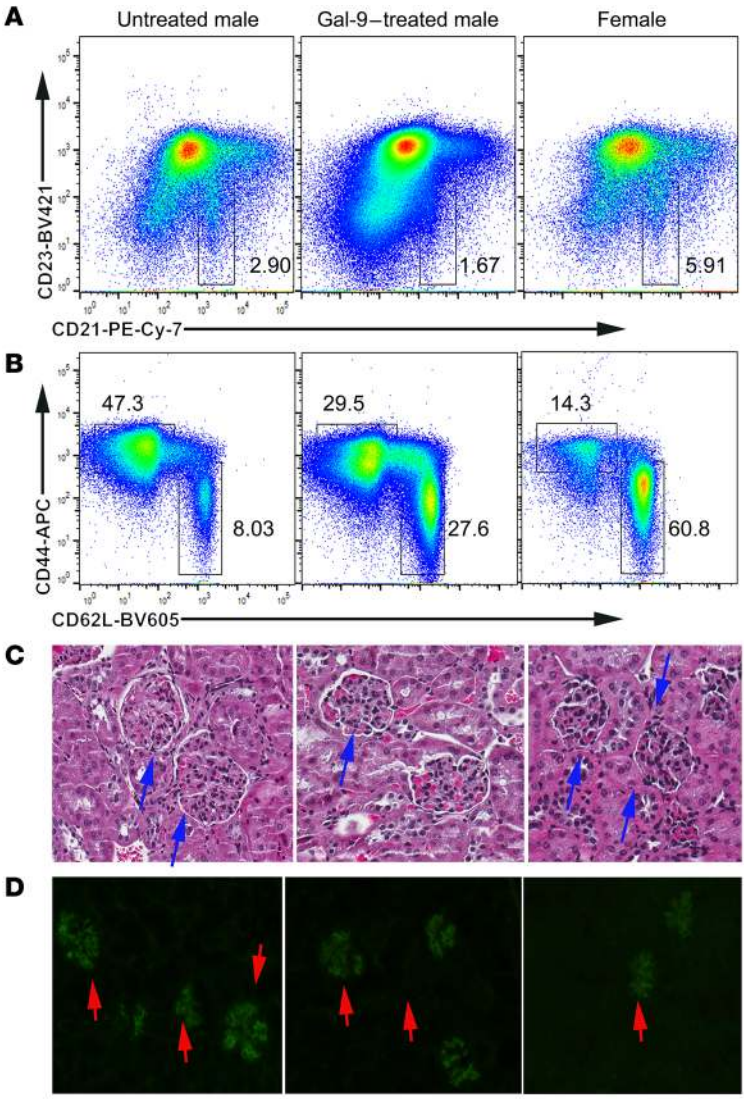

Figure 6. Therapeutic effects of Gal-9. Splenocytes from Gal-9–treated male, untreated male, and age-matched female littermates of BXSB/MpJ mice were analyzed for expression of different markers on CD19⁺ B cells and CD3⁺ T cells. (**A**) Representative flow cytometric plots of CD23 and CD21 expression on splenic B cells. (**B**) Representative flow cytometric plots of the expression of CD44 and CD62L on splenic CD4⁺ T cells. (**C**) Formalin-fixed kidney sections from 19-week-old Gal-9–treated and untreated control male BXSB/MpJ mice along with female littermates were stained for H&E. (**D**) Frozen kidney sections were stained for IgG. Representative images of 5 animals in each group. Individual glomeruli are marked with arrows. Original magnification, ×10.

TLR7/TLR9 ligands with and without Gal-9 for 24 hours and levels of IFN-α in culture supernatants were analyzed. TLR-induced production of IFN-α was inhibited by Gal-9 (Figure 7B). Similarly, Gal-9 completely abrogated the production of IFN-α and strongly reduced the production of TNF-α by human primary pDCs in response to various TLR7/TLR9 ligands, such as CpG-A, CpG-B, the imidazoquinolinone compound R848, influenza A RNA virus (Flu-A), and herpes simplex DNA virus (HSV-1) (Figure 7, C and D). Furthermore, Gal-9 inhibited production of IFN-α, TNF-α, and IL-6 in a dose-dependent manner (Supplemental Figure 5A). Importantly, other members of the galectin family failed to block TLR7/TLR9-mediated IFN-α production (Supplemental Figure 5B). The anti–Gal-9 antibody blocked the inhibitory effect of Gal-9, whereas the anti–Gal-1 antibody failed to do so, confirming the specificity of Gal-9 (Supplemental Figure 5C). It has previously been reported that Gal-9 inhibits the function of plasma cells (PCs), CD4⁺ T cells, and synovial fibroblasts by inducing apoptosis and cell death (23). However, we observed that the concentration of Gal-9 necessary to efficiently abrogate cytokine production only marginally affected the viability of pDCs (Supplemental Figure 5D). This observation suggested that the effect of Gal-9 on pDC function is independent of the apoptosis-inducing effect that has been shown previously (23). We further examined intracellular IFN-α and TNF-α levels in CpG-A–, Flu-A–, and HSV-1–activated pDCs in the presence of Gal-9 (Figure 7E). Consistently, Gal-9 treatment strongly decreased the amount of intracellular IFN-α and TNF-α in the viable population of activated pDCs. Phenotypic maturation of pDCs induced by TLR ligands was also affected by treatment with Gal-9. CpG-A– or Flu-A–induced upregulation of the costimulatory molecules CD80 and CD86 on pDCs was reduced by Gal-9 (Figure 7F and data not shown). In contrast, expression of inducible costimulatory ligand (ICOSL) was increased upon Gal-9 stimulation (Supplemental Figure 5E).

We evaluated the structural requirements for the inhibitory effect of Gal-9 on pDC function. The competitive substrate lactose that binds to the carbohydrate recognition domain (CRD) of Gal-9 diminished the effect of Gal-9 on pDCs, suggesting that the inhibitory effect of Gal-9 was mediated through CRDs (Figure 7G). Because of the uniqueness of the carbohydrate-binding profiles of N-terminal CRD and C-terminal CRD, it has been speculated that each CRD differentially contributes to the biological function of Gal-9. In fact, recent studies demonstrated that N-terminal CRD preferentially contributes to the activation of innate immune cells, such as DCs, whereas C-terminal CRD is mainly involved in the cell death signaling pathway in T cells (24). In contrast, the chemoattractant properties of Gal-9 require both the CRDs (25). To identify the structural requirements for Gal-9 activity by pDCs, we analyzed the inhibitory capacity of truncated forms of Gal-9 containing only 1 of its CRD domains. Neither the truncated form containing only the N-terminal CRD (CRD 1, aa 1–148) nor the truncated protein containing only the C-terminal CRD (CRD 2, aa 254-356) inhibited CpG-A– or Flu-A–induced inflammatory cytokine production, indicating that the inhibitory effect of Gal-9 on pDCs requires the presence of both CRDs (Figure 7H).

Gal-9 abrogates production of IFN-α and proinflammatory cytokines induced by ICs and NETs in human pDCs. Circulating ICs containing self-nucleic acid and NETs released by dying neutrophils in SLE patients physiologically trigger pDC activation in a TLR7- and TLR9-dependent manner (9, 10). The effect of Gal-9 on IC- and NET-mediated pDC activation was, therefore, investigated. ICs were isolated from the sera of SLE pediatric patients, whereas NETosis was elicited by exposing neutrophils from healthy donors to SLE-derived anti-ribonucleoprotein antibodies (anti–RNP-IgG) after a short pretreatment with IFN-α (10). Both purified SLE IC

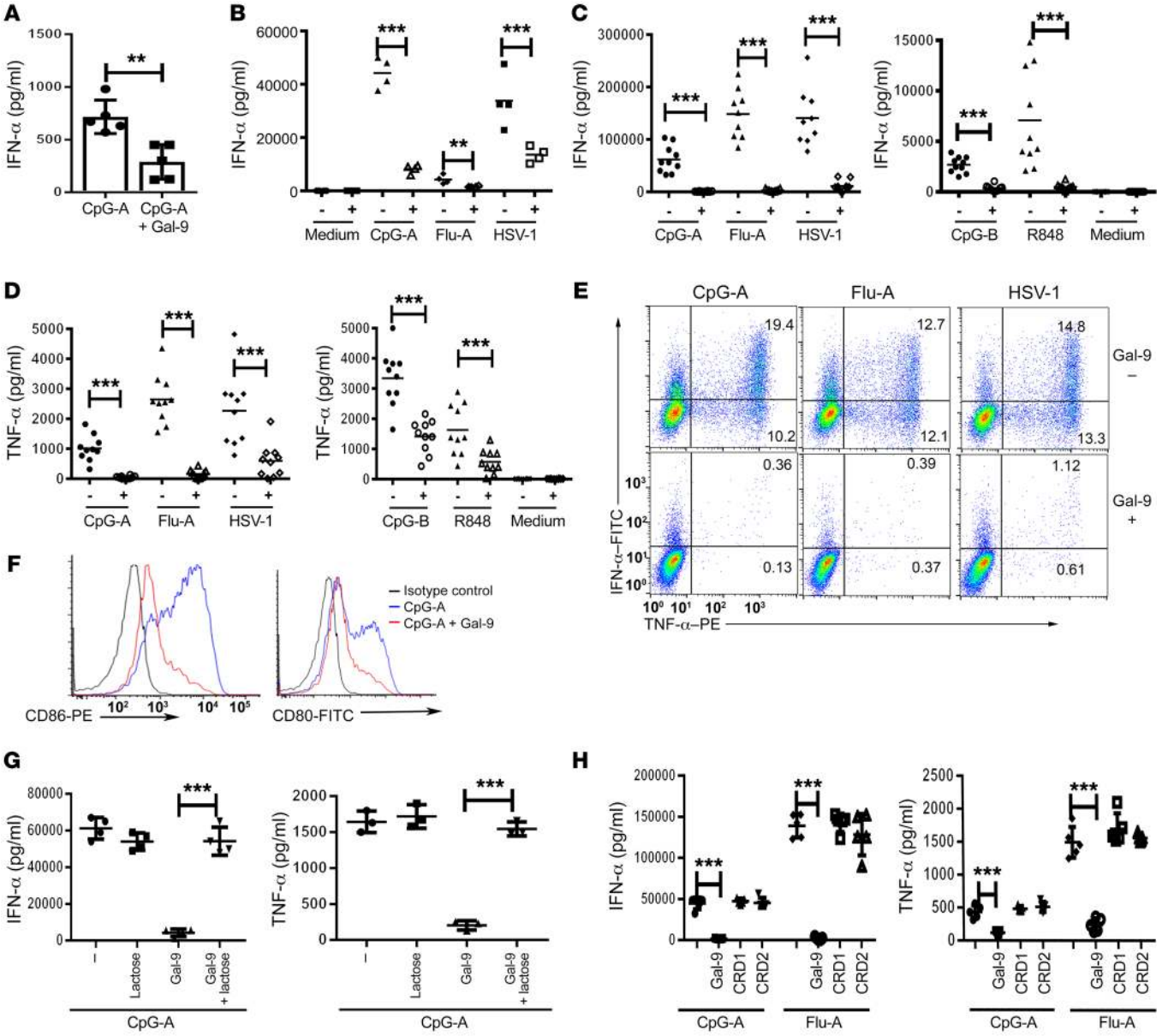

Figure 7. TLR-mediated pDC activation is inhibited by Gal-9. Serum levels of IFN-α in CpG-A– or CpG-A and Gal-9–injected C57BL/6 mice. Data are shown as mean ± SD (n = 5). (**B**) Murine pDCs were stimulated with CpG-A, Flu-A, and HSV-1 with or without Gal-9 for 24 hours, and the culture supernatants were analyzed for levels of IFN-α (n = 4). (**C** and **D**) Human pDCs were stimulated with the TLR7 and TLR9 ligands CpG-A, Flu-A, HSV-1, CpG-B, and R848 in the presence or absence of recombinant human Gal-9, and culture supernatants were analyzed for IFN-α (**C**) and TNF-α (**D**). Data shown are mean of 10 independent experiments. (**E**) Intracellular expression of human pDCs after stimulation with CpG-A, Flu-A, and HSV-1 with or without Gal-9. Numbers in quadrants are the percentage of cells. (**F**) Surface expression of CD80 and CD86 was analyzed after stimulation of pDCs with CpG-A, with or without Gal-9. (**G**) Human pDCs were stimulated with CpG-A and Gal-9 in the presence or absence of lactose, and the culture supernatants were analyzed for IFN-α and TNF-α. (**H**) Human pDCs were stimulated with CpG-A, Flu-A Gal-9, CRD1, or CRD2 in various combinations, and culture supernatants were analyzed for IFN-α and TNF-α. Data are shown as mean ± SD of 5 independent experiments. Unpaired Student's t test or Mann-Whitney U test with Welch's correction was used to test statistical significance. $^{**}P < 0.01$; $^{***}P < 0.001$ versus control without Gal-9.

and supernatants from netting neutrophils activated pDCs to produce high levels of IFN-α, but failed to do so when Gal-9 was added to the culture (Figure 8, A and B). The production of the proinflammatory cytokines TNF-α and IL-6 was also markedly inhibited in the presence of Gal-9.

Gal-9 inhibits TLR7/TLR9-mediated B cell activation and differentiation. Roles of TLR7 and TLR9 have been implicated in the differentiation of B cells into PCs and the generation of autoantibodies (14). Since Gal-9 inhibits TLR7/TLR9 signaling in pDCs, we next investigated the effect of Gal-9 on TLR-mediated B cell activation. Human B cells were stimulated with CpG-B with or without Gal-9 for 48 hours, and levels of IL-6 and IL-8 in culture supernatant were analyzed. Gal-9 inhibited CpG-B–mediated production of IL-6 and IL-8 by B cells in a dose-dependent manner (Figure 9A). Additionally, B cells were stimulated with either CpG-B or R848 and PC differentiation was assessed after 7 days.

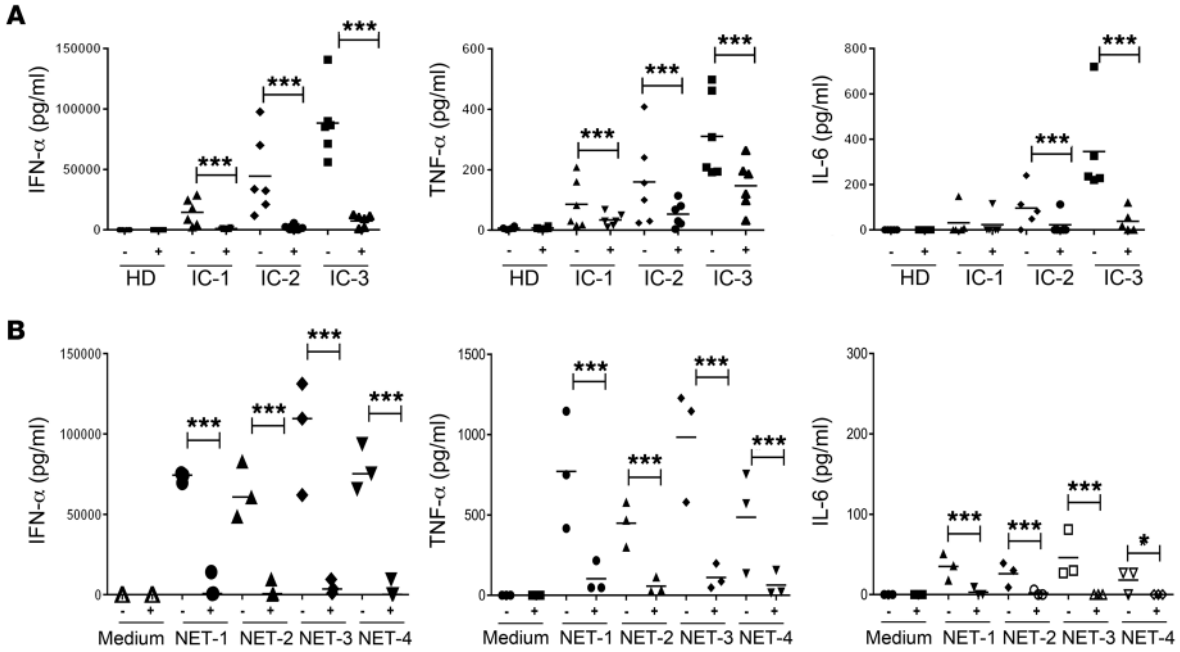

Figure 8. Gal-9 inhibits the IC- and NET-induced production of IFN-α, TNF-α, and IL-6 by pDCs. Human pDCs in the presence or absence of Gal-9 were stimulated with (**A**) IgG ICs isolated from the sera of SLE pediatric patients or (**B**) 30% culture supernatants from NET exposed to SLE-derived anti-RNP IgG. Culture supernatants were analyzed for IFN-α, TNF-α, and IL-6. Data shown are mean of 5 to 6 (**A**) and 3 (**B**) independent experiments without Gal-9. Unpaired Student's *t* test or Mann-Whitney *U* test with Welch's correction was used to test statistical significance. $^{*}P < 0.05$; $^{***}P < 0.001$ versus control.

Both CpG-B and R848 induced a population of $CD27^{hi}CD38^{hi}$ PCs (Figure 9B). Gal-9 inhibited PC generation in response to CpG-B and R848 by up to 80% and 82%, respectively (Figure 9, B and C, and Supplemental Figure 6). CpG-B also induced secretion of immunoglobulin, including IgG1, IgG2, and IgG3. Secretion of all of these IgG subclasses was reduced in the presence of Gal-9 (Figure 9D). In contrast, Gal-9 did not inhibit B cell differentiation in response to signals delivered through the BCR or CD40 (Supplemental Figure 6), highlighting a specific role of Gal-9 in the regulation of TLR-mediated B cell activation and differentiation.

Gal-9 impairs mTOR-dependent TLR activation. The receptor through which Gal-9 acts remains ambiguous. In order to identify the receptor for Gal-9 on the surface of pDCs, we first demonstrated the surface interaction of Gal-9 with pDCs by FACS analysis. Gal-9 bound to the surface of pDCs and B cells ex vivo in a dose-dependent manner (Figure 10A and Supplemental Figure 7A). Gal-9 also bound to the surface of pDCs and B cells in vivo (Supplemental Figure 7B). Interactions between galectins and their receptors are known to be dependent on carbohydrate chains of the receptors. Binding of Gal-9 to the surface of pDCs was inhibited by lactose, thus confirming that the binding of Gal-9 to the surface of pDCs is carbohydrate dependent (Figure 10B). Since T cell immunoglobulin and mucin-domain containing-3 (Tim-3) and CD44 both have been described as Gal-9 receptors on various cell types (17), the role of these receptors on pDCs was investigated. Although Tim-3 is expressed on the surface of pDCs, we found that both Tim-3–neutralizing antibodies and recombinant Tim-3 proteins were unable to block the inhibitory effect of Gal-9 on type I IFN production by pDCs (Supplemental Figure 8, A and B). Using coimmunoprecipitation and Western blotting, we confirmed that Gal-9 binds to CD44 expressed on pDCs (Figure 10C). Moreover, Gal-9 was also able to inhibit the interaction of anti-CD44 antibodies to the surface of pDCs and B cells (Figure 10D and Supplemental Figure 9). Binding of Gal-9 to pDCs was blocked in the presence of soluble recombinant CD44 (Figure 10E), and in those experimental conditions, Gal-9 failed to inhibit pDC activation in response to TLR ligands (Figure 10F). Further crosslinking of CD44 by anti-CD44 antibodies inhibited TLR-mediated pDC activation (Figure 10G). These results demonstrate that Gal-9 inhibits pDC function through CD44.

We further investigated the mechanism by which Gal-9–CD44 interaction inhibits TLR7/TLR9-mediated pDC function. CD44 is involved with phagocytosis and cytoskeletal movement (26). We first examined the effect of Gal-9 on CpG-A uptake by pDCs. Gal-9 did not affect the uptake of CpG-A (Figure 10H). Next, we examined the effect of Gal-9 on TLR trafficking. TLR7/TLR9 translocate from endoplasmic reticulum to endosome upon sensing of ligands such as CpG-A. CpG-A–induced trafficking of TLR9 to LAMP-1– or EEA-1–positive endosomes was not affected by Gal-9 (Supplemental Figure 10 and data not shown). These data indicate that Gal-9 does not disrupt TLR trafficking, but may instead interfere with downstream signal transduction of the TLR7/TLR9 pathway. Previous reports in T cells have demonstrated that the Gal-9–CD44 complex interacts with TGF-β receptor I (TGF-βRI), activates the Smad-3 pathway, and induces Treg differentiation (17). Interestingly, neither the TGF-βRI–blocking antibody nor Smad-3 inhibitors could reverse the inhibitory effect of Gal-9 (Supplemental Figure 11, A and B). This observation suggests that the inhibitory effect of Gal-9 is independent of the TGF-βRI/Smad-3 pathway. The CD44 ligation activates the Src kinase family of proteins (27). The Src kinase family

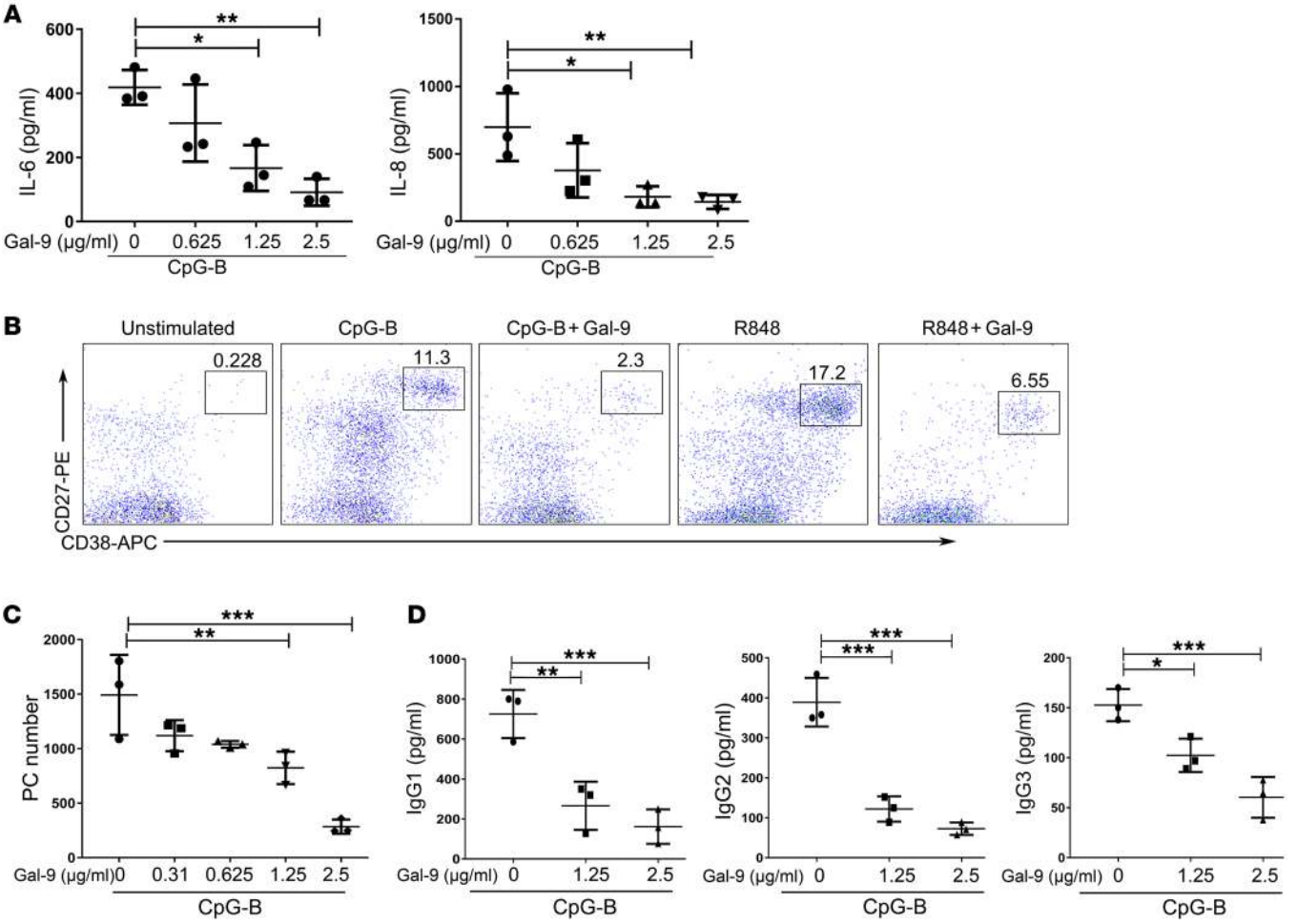

Figure 9. TLR7/TLR9-mediated B cell activation and differentiation are inhibited by Gal-9. Human peripheral B cells were stimulated with CpG-B or R848 in the presence or absence of Gal-9 as indicated. After 48 hours, the culture supernatants were analyzed for levels of IL-6 and IL-8 (**A**). On day 7 following activation, PCs were quantified by flow cytometry, identified as $CD19^{+/lo}CD27^{hi}CD38^{hi}$ cells. The number indicates percentage of PCs of total $CD19^{+}$ B cell population (**B**). Total $CD19^{+/lo}$ IgD^{-}, $CD27^{hi}$, $CD38^{hi}$ PC numbers (**C**) and IgG levels (**D**) were all determined after 7 days of culture. Data are representative of 3 independent donors. Mean ± SD of triplicate wells is shown. Kruskal-Wallis testing was performed, followed by Dunn's test for statistical significance. $^{*}P < 0.05$; $^{**}P < 0.01$; $^{***}P < 0.001$ versus control without Gal-9.

of proteins was reported to be activated by immunoreceptor tyrosine-based activation motif–signaling (ITAM-signaling) pathways, which inhibit TLR-mediated pDC activation (28). Shortly after Gal-9 stimulation, both Src and Syk family kinases were phosphorylated (Figure 10I). The intracellular domain of CD44 makes a complex with PI3K-AKT. It has been demonstrated that mTOR, p70S6K, and 4EBP-1 are phosphorylated downstream of PI3K-AKT activation and are required for TLR-mediated pDC activation (29). This pathway also plays a role in the generation of autoantibodies by B cells (30). p70S6K phosphorylation enhances protein translation and in turn phosphorylates 4EBP-1 and releases it from its translational repressor function (29). To assess the effect of Gal-9 on this pathway, human pDCs were stimulated with CpG-A, along with Gal-9, and phosphorylation of the above proteins was analyzed by Western blot. We observed that both phosphorylated mTOR and p70S6K were constitutively expressed in pDCs and slightly increased after CpG-A treatment, whereas phosphorylation of 4EBP-1 was upregulated. Gal-9 significantly reduced phosphorylation of mTOR, p70S6K, and 4EBP-1 (Figure 10J). Similar results were observed in B cells (Supplemental Figure 12). IRF7 phosphorylation was also inhibited by Gal-9 (data not shown). Together, these results suggest that Gal-9 impairs mTOR-dependent TLR activation.

Discussion

In this study, we show that Gal-9 inhibited TLR7- and TLR9-mediated activation of pDC and B cells. More specifically, Gal-9 blunted production of IFN-α, TNF-α, and IL-6 and also inhibited the expression of the costimulatory molecules CD80 and CD86 by pDCs. Additionally, Gal-9 abrogated cytokine production and differentiation of B cells into Ig-secreting PCs. This is the first report, to our knowledge, to demonstrate that Gal-9 regulates TLR7/TLR9-signaling pathways to inhibit pDC and B cell activation.

We demonstrate here that the inhibitory effect of Gal-9 on pDCs is mediated by its interaction with CD44 and is independent of Tim-3. Several molecules, such as Tim-3, PDI, and CD44, have been reported as receptors for Gal-9 (17, 31, 32). Tim-3, a Th1-specific cell-surface molecule, is the best-characterized receptor for Gal-9 (31), and interaction of Tim-3 with Gal-9 downregulates Th1

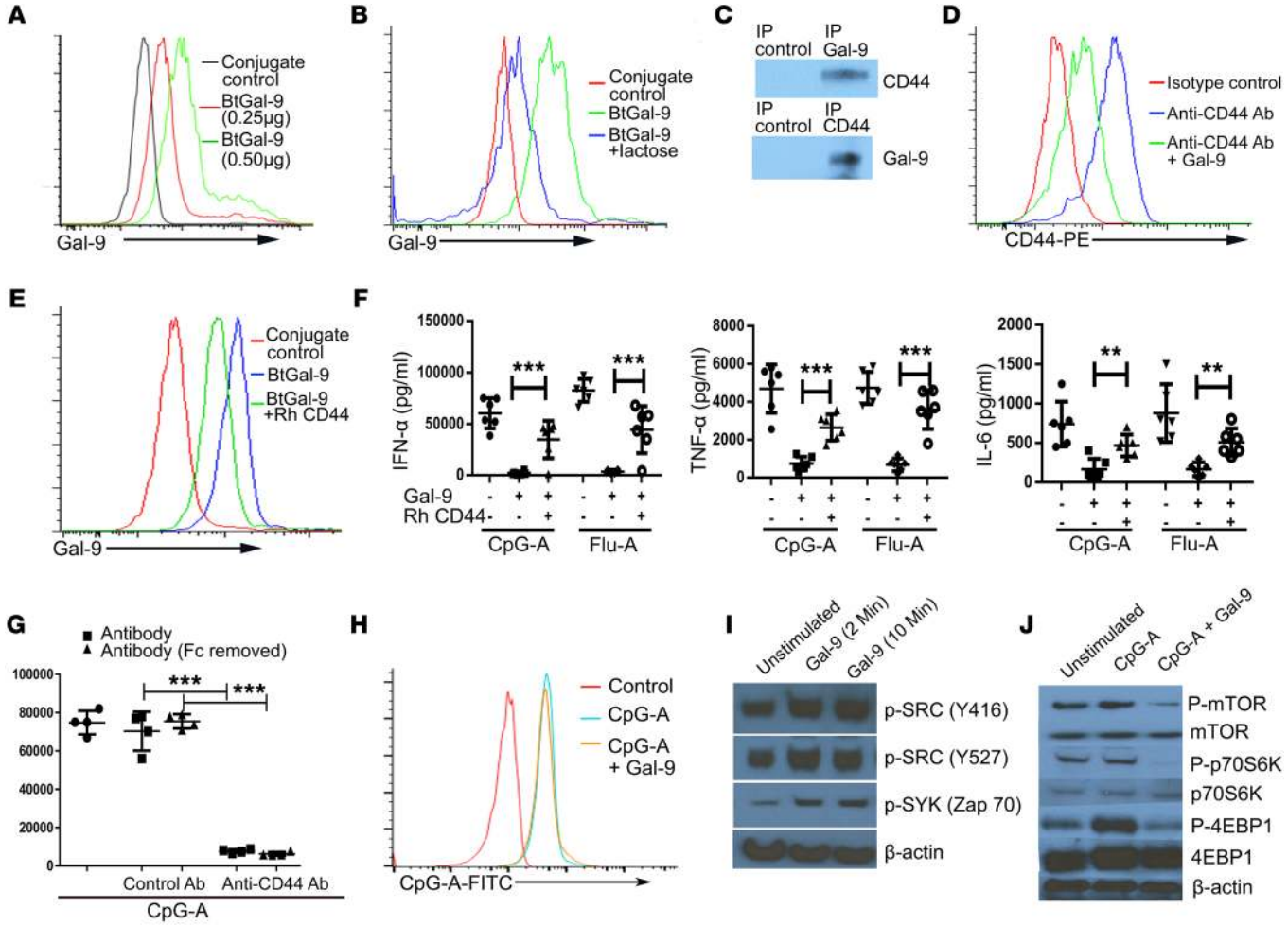

Figure 10. Gal-9 inhibited mTOR pathway through CD44 in pDCs. Human pDCs were incubated with different doses of biotinylated Gal-9 (BtGal-9), probed with avidin-FITC, and analyzed by FACS. (**A**) Representative overlaid histograms of different doses of biotinylated Gal-9 bound to the surface of pDCs. (**B**) pDCs were incubated with biotinylated Gal-9 with and without lactose, probed with avidin-FITC, and analyzed by FACS. (**C**) Gal-9–binding proteins from pDC lysates were immunoprecipitated and analyzed for the presence of CD44 (upper panel). CD44 was immunoprecipitated and analyzed for Gal-9 interaction in an immunoblot (lower panel). (**D**) Overlaid histograms of the binding of anti-CD44 antibodies to the surface of human pDCs with and without Gal-9. (**E**) Overlaid histograms of the binding of presaturated Gal-9 with CD44 recombinant protein (Rh CD44) to the surface of pDCs. Data are representative of 5 individual experiments. (**F**) Human pDCs were treated with either CpG-A or Flu-A with and without Gal-9 or presaturated Gal-9 with Rh CD44. Culture supernatants were analyzed for IFN-α, TNF-α, and IL-6. Mean ± SD for 6 independent experiments is shown. (**G**) Levels of IFN-α in supernatants of human pDCs treated with CpG-A, anti-CD44 antibodies, and control antibodies with and without Fc for 24 hours. Data are shown as the mean ± SD of 4 independent experiments. (**H**) Representative histogram showing CpG-A uptake by pDCs. Data are representative of 4 individual experiments. (**I**) Human primary pDCs were stimulated with Gal-9 for 2 and 10 minutes, and the cell lysates were analyzed by Western blotting. (**J**) Human primary pDCs were treated with CpG-A with or without Gal-9 for 15 minutes, and the cell lysates were analyzed by Western blotting. Data are representative of 5 independent experiments. Unpaired Student's *t* test or Mann-Whitney *U* test with Welch's correction was used to test the statistical significance. $^{**}P < 0.01$; $^{***}P < 0.001$ versus control without Gal-9.

(31) and CTL responses (33) by inducing apoptosis. The Tim-3/Gal-9 interaction also contributes to prolonged allograft survival and upregulation of antimicrobial immunity in vivo (34). However, there are other contradictory reports in the literature, which show that Gal-9 enhances T cell migration and suppresses Th17 development in a Tim-3–independent manner (35–37). In agreement with these latter observations, we found that the inhibitory effect of Gal-9 on pDCs is independent of Tim-3. CD44 is another receptor known to interact with Gal-9 and have multiple immunomodulatory effects (38). The Gal-9 and CD44 interaction regulates leukocyte migration during inflammation. Gal-9 is known to trigger osteoblast differentiation in a CD44-dependent mechanism (39, 40). A recent study also demonstrated that the Gal-9 and CD44 interaction promotes the function and stability of inducible Tregs by associating with TGF-βRI (41). In contrast, here we demonstrate that Gal-9 inhibits TLR7/TLR9 signaling in pDCs through CD44 in a TGF-βRI–Smad-3–independent manner.

TLR7 or TLR9 could not differentiate between host and pathogen-derived nuclear antigens. Compartmentalization of the above TLRs inside the cell limits their exposure to self-nuclear antigens commonly released by dead cells and maintains self-tolerance. In addition, several pDC-specific inhibitory receptors, such as ILT7, BDCA2, Siglec-H, and PTPRS, are present, which restrict the pathogenic IFN-α production. All these receptors,

except PTPRS, activate the Src kinase family of proteins through ITAM-containing adaptors. Here, we observed that Gal-9 activates Src kinase and inhibits TLR-mediated pDC activation. HSPG, the ligand of PTPRS, is an isoform of CD44 expressed by leukocytes. Similarly to what occurs with the above receptors, crosslinking of CD44 with anti-CD44 antibodies inhibited TLR-mediated pDC activation, suggesting a common mechanism at play for controlling unabated IFN production. The inhibitory effect of the Gal-9–CD44 interaction might play a role in maintaining immune homeostasis.

The mTOR/p70S6K/4EBP-1 pathway plays a pivotal role in TLR signaling. TLR-MYD88 complex activates PI3K-AKT, which in turn phosphorylates mTOR. p70S6K and 4EBP-1 are phosphorylated downstream of mTOR and initiate the translation process (29). Phosphorylated mTOR is also recruited directly by the MYD88 scaffold protein, resulting in activation of IRF-5 and IRF-7, induction of inflammatory pathways, and production of type-1 IFN (42). This pathway is indispensable for TLR-induced type-1 IFN and autoantibody production by pDCs and B cells (29, 30). TLR-mediated phosphorylation of mTOR, p70S6K, and 4EBP-1 was inhibited in both pDCs and B cells upon Gal-9 treatment. Although the precise mechanism of this inhibition is not clear, activation of CD44 through Gal-9 might play a role. The intracellular domain of CD44 is known to engage the PI3K-AKT complex upon activation (43), which may limit the recruitment of mTOR to the TLR-MYD88 complex and inhibit TLR-mediated IRF5 and IRF7 activation. Further, we have observed that Gal-9 treatment did not affect CpG-A–mediated TLR9 trafficking to the endosomes and AKT activation, while phosphorylation of mTOR and downstream p70S6K and 4EBP-1 was inhibited. This suggests that Gal-9–CD44 interaction inhibits the TLR pathway downstream of AKT. It has been demonstrated that CD44 activation upregulates Rho-GTPase (44). GTPase plays an important role in negative regulation of mTOR. Hence, Gal-9–CD44 interaction might inhibit mTOR phosphorylation through multiple mechanisms by direct engagement of PI3K-AKT and by indirect inactivation of mTOR by GTPase. We and others observed that mTOR is constitutively phosphorylated in pDCs (29), which may facilitate quick IFN response against viral infections. Since unabated IFN secretion leads to autoimmune manifestations, regulation of this pathway is important. Viral infections are known to trigger Gal-9 secretion by vascular endothelial cells (25, 45). By inhibiting mTOR phosphorylation, Gal-9 might maintain a fine balance of IFN response and thereby skew the host response away from autoimmunity, toward neutralization of viral infections. Recently, it was demonstrated that Gal-9 inhibits dectin-1 signaling; however, the mechanism remains unexplained. Since mTOR signaling is an integral component of dectin-1–mediated activation, the inhibitory effect of Gal-9 on this pathway might be attributed to its ability to attenuate mTOR signaling (46).

The role of pDC and type-1 IFN in initiating autoimmune manifestations and driving the differentiation of autoreactive B cells and T cells has been demonstrated (7, 12, 47). Blocking of IFN signaling by administration of anti-IFN-α/β receptor (IFNAR) or anti-IFN antibodies at the initial stage of the disease has been shown to effectively improve lupus symptoms, whereas it fails to ameliorate the disease when administered at the late stage (48). Further, there is evidence in the literature to suggest that early transient depletion of pDC reduces clinical parameters of lupus, including IFN signatures, even in the presence of repopulated normal pDC populations at the later stage of the disease (11). Consistent with these observations, we found that administration of Gal-9 at the early onset of the disease inhibits lupus pathogenesis, whereas it fails to do so at the late stage of the disease. Thus, our findings here reinforce the previous view that contribution of pDCs and type-1 IFN is limited to the initiation and progression of the disease in these murine models.

$CD4^+$ T cells potentially play a role in SLE by stimulating B cells to differentiate and proliferate and by promoting class switching of autoantibodies (49). In fact, an increased frequency of activated $CD4^+$ T cells has been reported in both SLE patients and BXSB mice (11, 48). In our study, in vivo treatment of Gal-9 remarkably decreased the frequency of activated $CD4^+$ T cells, marked by expression of CD44 and CD69. Additionally, the frequency of $CD8^+$ T cells that are activated in an IFN-dependent manner during lupus (48) was also observed to decrease upon Gal-9 treatment. Thus, multiple mechanisms may be involved in the inhibitory effects of Gal-9 in animal models, including direct inhibition of activated T cells. However, it has been shown that type I IFNs produced by pDCs play an essential role in regulating the generation and function of adaptive immune responses by promoting the IFN-γ production by $CD4^+$ and $CD8^+$ T cells (50). Therefore, inhibition of type I IFNs by Gal-9 during the early onset of autoimmunity might contribute to limiting the downstream activation of aberrant $CD4^+$ and $CD8^+$ T cells. Interestingly, Gal-9 upregulated ICOSL expression by pDCs, although CD80 and CD86 expression was downregulated. Since ICOSL on pDCs stimulates naive $CD4^+$ T cells to differentiate into IL-10–producing Tregs (51), it appears that Gal-9 might play an important role in the induction of Tregs through pDCs.

ABCs are an unusual population of B cells that are accumulated with age in normal humans and mice or autoimmune-prone animals and patients (52). Recent studies showed that TLR7 and TLR9 signaling and type I IFNs play a major role in the generation and accumulation of ABCs (48). We demonstrate here that Gal-9 treatment limited the accumulation of ABCs in BXSB/MpJ mice, suggesting that inhibition of TLR7/TLR9 signaling by Gal-9 affects aberrant B cell differentiation. IFN-α secreted by pDCs induces B cells to mature into plasmablasts, and IL-6 differentiates plasmablasts into PCs (53). In addition to differentiation, IFN-α induces the break of B cell tolerance to nucleic acids and promotes anti-nucleic acid antibody production (54). PCs are elevated in lupus patients (55), and an increased frequency of PCs was also observed in the lupus-prone MRL/lpr mice (20). In the BXSB/MpJ mice, we did not observe a higher prevalence of PCs, which is consistent with previous descriptions of the model (11, 12). We did observe, however, decreased levels of pathogenic IgG2c autoantibodies upon Gal-9 administration. Thus, it is plausible that Gal-9–dependent inhibition of TLR7/TLR9 signaling blocks the differentiation of autoreactive B cells without a global effect on PC populations.

In conclusion, we report a function of Gal-9 in regulating TLR7/TLR9 signaling in pDCs and B cells. Importantly, blocking of IC- and NET-mediated pDC activation by Gal-9 highlights its

physiological importance in lupus. Recently, our group demonstrated the role of IgE-IC in the activation of pDC (56). Gal-9 binds to IgE and inhibits IC formation (57), which highlights an alternative mechanism by which pDC activation is inhibited by Gal-9. Findings of the present study, however, added a dimension to our understanding about the role of Gal-9 in regulating autoimmune responses. Considering the importance of TLR7/TLR9 signaling in the initiation and progression of autoimmunity, identification of Gal-9 as an inhibitor of these pathways in pDCs and B cells denotes the potential implication of Gal-9 in blocking IFN-driven autoimmune disorders.

Methods

Chemicals and antibodies. Galectins 1–9 used for all in vitro experiments were obtained from R&D Systems. Gal-9 obtained from GalPharma was used for in vivo experiments. CpG DNAs and R848 were purchased from InvivoGen. ICs and NETs were gifts from V. Pascaul and S. Caielli (Baylor Institute of Immunology Research). The Annexin V kit was obtained from BD Biosciences.

Anti-human antibodies used were as follows: anti-CD11c (B-ly6), anti-CD4 (RPA-T4), anti-CD3 (HIT3a), anti-CD14 (MØP9), anti-CD15 (HI98), anti-CD16 (3G8), anti-CD19 (HIB19), anti-CD20 (2H7), anti-CD56 (B159), and anti-CD123 (6H6). Anti-mouse antibodies used were as follows: anti-CD19 (1D3), anti-CD21 (eBio8D9), anti-CD23 (B3B4), anti-IgM (11/41), anti-AA4.1 (AA4.1), anti-IgD (1126c.2a),anti-CD138 (281.2), anti-CD3 (145 2c11), anti-CD4 (Gk1.5), anti-CD8 (53-6.7), anti-CD44 (IM7), anti-CD62L (MEL-14), anti-CD69 (H12F3), anti-B220 (RA3-6B2), anti–PDCA-1 (eBio129c), anti–Siglec-H (eBio44c), anti-CD80 (16 10-A1), and anti-CD86 (GL-1). These antibodies, with various fluorescent tags, were purchased from BD Biosciences. Anti-human CD16 (3G8), anti-human CD19 (HIB19) were purchased from Biolegend and anti-mouse CD21 (eBio8D9), anti-mouse PDCA-1 (eBio129c) and anti-mouse Siglec-H (eBio44c) were obtained from eBiosciences.

Mice and treatment. BXSB/MpJ and NZB/W F1 mice were purchased from the Jackson Laboratory and housed in the animal facility at MedImmune. BXSB male mice 8 weeks of age were treated with Gal-9 at 1 mg/kg body weight 3 times per week up to 18 weeks. Age-matched untreated males and females were considered as controls to compare clinical parameters of lupus. Similarly, female NZB/W F1 mice were treated with Gal-9 for 11 weeks beginning at 20 weeks of age. Age-matched untreated females and males were considered as controls to compare clinical parameters of lupus. At the end of the treatment, mice were sacrificed and blood was collected by heart puncture. Sera were stored at –80°C. Spleens were analyzed for weight, number of splenocytes, and immune cell phenotypes. C57BL/6 mice were obtained from Harlan Laboratories and housed in the animal facility of MedImmune. CpG-A encapsulated with DOTAP with or without Gal-9 was administered.

Isolation and culture of pDCs. Human pDCs were isolated from commercially obtained buffy coats or whole blood collected from healthy volunteers recruited by the MedImmune blood donor program. PBMCs were isolated by density gradient centrifugation using Histopaque (MilliporeSigma), and pDCs were enriched using a human pDC enrichment kit (STEMCELL Technologies), followed by FACS to specifically isolate $CD3^-$, $CD14^-$, $CD19^-$, $CD20^-$, $CD16^-$, $CD56^-$, $CD11c^-$, $CD4^+$, and $CD123^+$. The purified cells were plated at 0.25 to 0.5×10^5 cells/well in 100 μl in U bottom 96-well culture plates. The cells were stimulated with CpG-A (0.2 μm), CpG-B (0.2 μm), R848 (10 μg/ml), Flu-A (1×10^5 PFU), and ICs and NETs with and without Gal-9 (2.5 μg/ml) for 24 hours. The cells were analyzed for CD80 and CD86 expression by FACS. The culture supernatants were analyzed for levels of IFN-α, TNF-α, and IL-6.

Isolation and culture of human B cells. Human blood was collected from healthy donors. B cells were negatively selected using a kit from Stem Cell Technology according to the manufacturer's instructions. Purified B cells were cultured at a density of 0.5 to 1.0×10^5 B cells per well in 96-well round-bottom plates and were stimulated with either CpG-B (1 μg/ml, Invivogen) or R848 (10 μg/ml). Alternatively, B cells were stimulated with anti-CD40 (R&D Systems, 0.1 μg/ml) and IL-21 (MedImmune, 33 ng/ml) in the presence or absence of anti-IgM $F(ab')_2$ (5 ug/ml, Jackson ImmunoResearch Laboratories). Gal-9 was included (up to 2.5 μg/ml) at the initiation of culture. Supernatants were collected at 48 hours for cytokine evaluation and at 7 days for quantitation of Ig. After 7 days of activation, PC differentiation was assessed by flow cytometry.

FACS analysis. Human pDCs were stained with fluorescent-labeled anti-human CD80, CD86, and ICOSL antibodies and were analyzed by FACS. Appropriate isotype controls were used.

Murine splenocytes were harvested, and the cell suspension was passed through a 70-micron nylon mesh to avoid cell clumps. RBCs were lysed using ACK lysis buffer. The cells were stained with B cell (CD19, CD21, CD23, IgM, IgD), T cell (CD3, CD4, CD8, CD44, CD62L, CD69), and pDC (B220, PDCA-1, Siglec-H, CD80, CD86) markers. Dead cells were excluded during FACS analysis using LIVE/DEAD Fixable Blue Dead Cell Stain Kit (Life Technologies). Human B cells were stained with the following antibodies: anti-CD19 (HIB19; Biolegend), anti-IgD (IA6-2; BD Biosciences), anti-CD38 (HB7; BD Biosciences), and anti-CD27 (M-T271; Biolegend). Analysis was performed using the BD LSR II (BD Biosciences) and FlowJo software (FlowJo).

Quantification of cytokines. Culture supernatants were analyzed for levels of IFN-α, TNF-α, IL-6, and IL-8 by a sandwich ELISA using commercially available ELISA kits (Mabtech) according to the manufacturer's instructions.

SDS-PAGE and Western blotting. Human pDCs and B cells were pretreated with Gal-9 for 15 minutes followed by CpG-A treatment for 15 minutes. Cells were lysed with LDL sample buffer containing protease inhibitors and then separated by 4% to 12% SDS-PAGE, followed by blotting into nitrocellulose membrane. Then the membrane was blocked with 3% BSA-TBST and probed with different antibodies. The antibodies used for immunoblotting were anti-mTOR (catalog 2983), anti-phosphorylated mTOR (S2448) (catalog 5536), anti-p70S6K (catalog 9202), anti-phosphorylated p70S6K (T389) (catalog 9234), anti–4E-BP1 (catalog 9452), and anti-phosphorylated 4E-BP1(S65) (catalog 9451). These antibodies were obtained from Cell Signaling Technology.

Proteinuria estimation. Proteinuria levels in 19-week-old male BXSB/MpJ mice with and without Gal-9 treatment and female littermates were quantified using Albustix strips (Bayer) according to the manufacturer's instructions.

Gene-expression analysis. RNA from flash-frozen kidney tissues of 19-week-old male BXSB/MpJ mice with and without Gal-9 treatment and female littermates were isolated using the RNeasy Mini Kit (QIAGEN), and c-DNA was prepared using a SuperScript III c-DNA Synthesis Kit (Life Technologies). TaqMan Fast Advanced Master Mix was used to ana-

lyze the expression of Mx-1 (Mm00487796_m1), OAS3 (Mm00460944_m1), IRF7 (Mm00519791_g1), and IFIT1 (Mm00515153_m1). Amplification data were analyzed using RQ manager (Applied Biosystems), and fold changes were calculated using GAPDH.

Quantification of antibodies. Serum autoantibodies were quantified by ELISA using isotype-specific antibodies, and 96-well Nunc-MaxiSorp ELISA plates were coated with goat anti-mouse/human IgG (H+L) or nuclear antigens (ssDNA, dsDNA, or chromatins) and incubated with mouse serum or culture supernatants. Antibody levels were estimated by probing with AP-conjugated specific isotype antibodies. Antibodies were purchased from Southern Biotech.

Histopathology and immunohistochemical staining. Formalin-fixed kidney sections were stained with H&E. Kidneys of treated animals were removed at the indicated ages. Tissues were frozen in OCT, and blocks were stored at –70°C until sectioning. Frozen tissues were sectioned (5 μm thickness), fixed in acetone, blocked with 10% FBC, and stained with IgG-FITC. Two to three cryosections per mouse were evaluated.

For further information, see Supplemental Methods.

Statistics. For comparison between multiple groups, assumptions were tested for each data set prior to final analysis. If assumptions were satisfied, ANOVA was performed, followed by Dunnett's test for multiple comparison. If assumptions were not satisfied, Kruskal-Wallis testing was performed, followed by Dunn's test for multiple comparison. Adjusted P values were estimated for all pairwise testing. Two-sided testing was performed at the 0.05 level. Unpaired Student's t test (2-tailed) or Mann-Whitney U test with Welch's correction was used for comparison between 2 groups based on the distribution of data. All statistical analysis was performed using GraphPad Prism 7 software. $P < 0.05$ was considered statistically significant, with 95% CI.

Study approval. The present studies in animals and humans were reviewed and approved by the Chesapeake Institutional Review Board (Columbia, Maryland, USA) and the IRB of the Baylor Institute of Immunology Research. Adult human blood was collected from healthy donors following informed consent as approved by MedImmune's IRB and the Baylor Institute of Immunology Research. All animal protocols were done in accordance with and approved by MedImmune's Institutional Animal Use and Care Committees.

Author contributions

YJL conceived the idea and supervised the project. SKP, SH, and MAS designed the animal experiments. SKP and VF performed the experiments. JLK and SKP designed and performed the human B cell studies. EV, RNH, and SKP performed histopathology and microscopy. SKP wrote the manuscript. RE, MAS, and YJL edited and gave a final shape to the manuscript. RK gave critical comments on the manuscript.

Acknowledgments

We thank V. Pascaul and Simone Caielli for providing NETs and ICs and Yoichiro Ohne, Musheng Bao, T. Kim, Leiyun Weng, and Haryuki Fujita for laboratory support. We are thankful to Wilson George and the staff of the animal facility for excellent technical assistance with animal experiments. Research was conducted at MedImmune and the Baylor Institute of Immunology Research.

Address correspondence to: Yong-jun Liu, Sanofi, 640 Memorial Drive, Cambridge, Massachusetts 02139, USA. Phone: 617.665.4577; Email: yong-jun.liu@sanofi.com. Or to: Rachel Ettinger, Viela Bio, One MedImmune Way, Gaithersburg, Maryland 20878, USA. Phone: 301.398.5756; Email: ettingerr@vielabio.com.

MAS's present address is: Bristol-Myers Squibb, Lawrence Township, New Jersey, USA.

YJL's present address is: Sanofi, Cambridge, Massachusetts, USA.

RE and JLK's present address is: Viela Bio, Gaithersburg, Maryland, USA.

1. Marshak-Rothstein A. Toll-like receptors in systemic autoimmune disease. *Nat Rev Immunol*. 2006;6(11):823–835.
2. Banchereau J, Pascual V. Type I interferon in systemic lupus erythematosus and other autoimmune diseases. *Immunity*. 2006;25(3):383–392.
3. Toong C, Adelstein S, Phan TG. Clearing the complexity: immune complexes and their treatment in lupus nephritis. *Int J Nephrol Renovasc Dis*. 2011;4:17–28.
4. Rönnblom L, Pascual V. The innate immune system in SLE: type I interferons and dendritic cells. *Lupus*. 2008;17(5):394–399.
5. Green NM, Marshak-Rothstein A. Toll-like receptor driven B cell activation in the induction of systemic autoimmunity. *Semin Immunol*. 2011;23(2):106–112.
6. Reizis B, Bunin A, Ghosh HS, Lewis KL, Sisirak V. Plasmacytoid dendritic cells: recent progress and open questions. *Annu Rev Immunol*. 2011;29:163–183.
7. Swiecki M, Colonna M. The multifaceted biology of plasmacytoid dendritic cells. *Nat Rev Immunol*. 2015;15(8):471–485.
8. Bao M, Liu YJ. Regulation of TLR7/9 signaling in plasmacytoid dendritic cells. *Protein Cell*. 2013;4(1):40–52.
9. Gilliet M, Cao W, Liu YJ. Plasmacytoid dendritic cells: sensing nucleic acids in viral infection and autoimmune diseases. *Nat Rev Immunol*. 2008;8(8):594–606.
10. Garcia-Romo GS, et al. Netting neutrophils are major inducers of type I IFN production in pediatric systemic lupus erythematosus. *Sci Transl Med*. 2011;3(73):73ra20.
11. Rowland SL, et al. Early, transient depletion of plasmacytoid dendritic cells ameliorates autoimmunity in a lupus model. *J Exp Med*. 2014;211(10):1977–1991.
12. Sisirak V, et al. Genetic evidence for the role of plasmacytoid dendritic cells in systemic lupus erythematosus. *J Exp Med*. 2014;211(10):1969–1976.
13. Heer AK, et al. TLR signaling fine-tunes anti-influenza B cell responses without regulating effector T cell responses. *J Immunol*. 2007;178(4):2182–2191.
14. Giltiay NV, et al. Overexpression of TLR7 promotes cell-intrinsic expansion and autoantibody production by transitional T1 B cells. *J Exp Med*. 2013;210(12):2773–2789.
15. Ehlers M, Fukuyama H, McGaha TL, Aderem A, Ravetch JV. TLR9/MyD88 signaling is required for class switching to pathogenic IgG2a and 2b autoantibodies in SLE. *J Exp Med*. 2006;203(3):553–561.
16. Golden-Mason L, et al. Galectin-9 functionally impairs natural killer cells in humans and mice. *J Virol*. 2013;87(9):4835–4845.
17. Wu C, et al. Galectin-9–CD44 interaction enhances stability and function of adaptive regulatory T cells. *Immunity*. 2014;41(2):270–282.
18. Arikawa T, et al. Galectin-9 ameliorates immune complex-induced arthritis by regulating Fc gamma R expression on macrophages. *Clin Immunol*. 2009;133(3):382–392.
19. Seki M, et al. Galectin-9 suppresses the generation of Th17, promotes the induction of regulatory T cells, and regulates experimental autoimmune arthritis. *Clin Immunol*. 2008;127(1):78–88.
20. Moritoki M, et al. Galectin-9 ameliorates clinical severity of MRL/lpr lupus-prone mice by inducing plasma cell apoptosis independently of Tim-3. *PLoS One*. 2013;8(4):e60807.
21. Barrat FJ, Meeker T, Chan JH, Guiducci C, Coffman RL. Treatment of lupus-prone mice with a dual inhibitor of TLR7 and TLR9 leads to reduction of autoantibody production and amelioration of disease symptoms. *Eur J Immunol*. 2007;37(12):3582–3586.

22. Baechler EC, et al. Interferon-inducible gene expression signature in peripheral blood cells of patients with severe lupus. *Proc Natl Acad Sci U S A*. 2003;100(5):2610–2615.
23. Liu FT, Rabinovich GA. Galectins as modulators of tumour progression. *Nat Rev Cancer*. 2005;5(1):29–41.
24. Li Y, et al. The N- and C-terminal carbohydrate recognition domains of galectin-9 contribute differently to its multiple functions in innate immunity and adaptive immunity. *Mol Immunol*. 2011;48(4):670–677.
25. Hirashima M, et al. Galectin-9 in physiological and pathological conditions. *Glycoconj J*. 2002;19(7–9):593–600.
26. Vachon E, et al. CD44-mediated phagocytosis induces inside-out activation of complement receptor-3 in murine macrophages. *Blood*. 2007;110(13):4492–4502.
27. Thorne RF, Legg JW, Isacke CM. The role of the CD44 transmembrane and cytoplasmic domains in co-ordinating adhesive and signalling events. *J Cell Sci*. 2004;117(pt 3):373–380.
28. Cao W, et al. Plasmacytoid dendritic cell-specific receptor ILT7-Fc epsilonRI gamma inhibits Toll-like receptor-induced interferon production. *J Exp Med*. 2006;203(6):1399–1405.
29. Cao W, et al. Toll-like receptor-mediated induction of type I interferon in plasmacytoid dendritic cells requires the rapamycin-sensitive PI(3)K-mTOR-p70S6K pathway. *Nat Immunol*. 2008;9(10):1157–1164.
30. Kobayashi T, et al. The histidine transporter SLC15A4 coordinates mTOR-dependent inflammatory responses and pathogenic antibody production. *Immunity*. 2014;41(3):375–388.
31. Zhu C, et al. The Tim-3 ligand galectin-9 negatively regulates T helper type 1 immunity. *Nat Immunol*. 2005;6(12):1245–1252.
32. Bi S, Hong PW, Lee B, Baum LG. Galectin-9 binding to cell surface protein disulfide isomerase regulates the redox environment to enhance T-cell migration and HIV entry. *Proc Natl Acad Sci U S A*. 2011;108(26):10650–10655.
33. Sharma S, et al. T cell immunoglobulin and mucin protein-3 (Tim-3)/Galectin-9 interaction regulates influenza A virus-specific humoral and CD8 T-cell responses. *Proc Natl Acad Sci U S A*. 2011;108(47):19001–19006.
34. Jayaraman P, et al. Tim3 binding to galectin-9 stimulates antimicrobial immunity. *J Exp Med*. 2010;207(11):2343–2354.
35. Leitner J, Rieger A, Pickl WF, Zlabinger G, Grabmeier-Pfistershammer K, Steinberger P. TIM-3 does not act as a receptor for galectin-9. *PLoS Pathog*. 2013;9(3):e1003253.
36. Golden-Mason L, et al. Galectin-9 functionally impairs natural killer cells in humans and mice. *J Virol*. 2013;87(9):4835–4845.
37. Oomizu S, et al. Galectin-9 suppresses Th17 cell development in an IL-2-dependent but Tim-3-independent manner. *Clin Immunol*. 2012;143(1):51–58.
38. Katoh S, et al. Galectin-9 inhibits CD44-hyaluronan interaction and suppresses a murine model of allergic asthma. *Am J Respir Crit Care Med*. 2007;176(1):27–35.
39. Tanikawa R, Tanikawa T, Hirashima M, Yamauchi A, Tanaka Y. Galectin-9 induces osteoblast differentiation through the CD44/Smad signaling pathway. *Biochem Biophys Res Commun*. 2010;394(2):317–322.
40. Kawana H, et al. CD44 suppresses TLR-mediated inflammation. *J Immunol*. 2008;180(6):4235–4245.
41. Wu C, et al. Galectin-9–CD44 interaction enhances stability and function of adaptive regulatory T cells. *Immunity*. 2014;41(2):270–282.
42. Schmitz F, et al. Mammalian target of rapamycin (mTOR) orchestrates the defense program of innate immune cells. *Eur J Immunol*. 2008;38(11):2981–2992.
43. Toole BP. Hyaluronan: from extracellular glue to pericellular cue. *Nat Rev Cancer*. 2004;4(7):528–539.
44. Bourguignon LY. Hyaluronan-mediated CD44 activation of RhoGTPase signaling and cytoskeleton function promotes tumor progression. *Semin Cancer Biol*. 2008;18(4):251–259.
45. Ishikawa A, et al. Double-stranded RNA enhances the expression of galectin-9 in vascular endothelial cells. *Immunol Cell Biol*. 2004;82(4):410–414.
46. Daley D, et al. Dectin 1 activation on macrophages by galectin 9 promotes pancreatic carcinoma and peritumoral immune tolerance. *Nat Med*. 2017;23(5):556–567.
47. Santiago-Raber ML, et al. Type-I interferon receptor deficiency reduces lupus-like disease in NZB mice. *J Exp Med*. 2003;197(6):777–788.
48. Baccala R, Gonzalez-Quintial R, Schreiber RD, Lawson BR, Kono DH, Theofilopoulos AN. Anti-IFN-α/β receptor antibody treatment ameliorates disease in lupus-predisposed mice. *J Immunol*. 2012;189(12):5976–5984.
49. Hoffman RW. T cells in the pathogenesis of systemic lupus erythematosus. *Clin Immunol*. 2004;113(1):4–13.
50. Huber JP, Farrar JD. Regulation of effector and memory T-cell functions by type I interferon. *Immunology*. 2011;132(4):466–474.
51. Ito T, et al. Plasmacytoid dendritic cells prime IL-10-producing T regulatory cells by inducible costimulator ligand. *J Exp Med*. 2007;204(1):105–115.
52. Rubtsov AV, et al. Toll-like receptor 7 (TLR7)-driven accumulation of a novel CD11c^{+} B-cell population is important for the development of autoimmunity. *Blood*. 2011;118(5):1305–1315.
53. Jego G, Palucka AK, Blanck JP, Chalouni C, Pascual V, Banchereau J. Plasmacytoid dendritic cells induce plasma cell differentiation through type I interferon and interleukin 6. *Immunity*. 2003;19(2):225–234.
54. Fairhurst AM, et al. Systemic IFN-α drives kidney nephritis in B6.Sle123 mice. *Eur J Immunol*. 2008;38(7):1948–1960.
55. Liu Z, Zou Y, Davidson A. Plasma cells in systemic lupus erythematosus: the long and short of it all. *Eur J Immunol*. 2011;41(3):588–591.
56. Henault J, et al. Self-reactive IgE exacerbates interferon responses associated with autoimmunity. *Nat Immunol*. 2016;17(2):196–203.
57. Niki T, et al. Galectin-9 is a high affinity IgE-binding lectin with anti-allergic effect by blocking IgE-antigen complex formation. *J Biol Chem*. 2009;284(47):32344–32352.